Vol 18 No 9, September 2009
1674-1056/2009/18(09)/3677-10

Chinese Physics B

© 2009 Chin. Phys. Soc.
and IOP Publishing Ltd

Tunable thermal entanglement in an effective spin-star system using coupled microcavities*

Yang Wan-Li(杨万里)[a)b)], Wei Hua(魏 华)[a)b)],
Feng Mang(冯 芒)[a)†], and An Jun-Hong(安钧鸿)[c)d)]

[a)] *State Key Laboratory of Magnetic Resonance and Atomic and Molecular Physics, Wuhan Institute of Physics and Mathematics, Chinese Academy of Sciences, Wuhan* 430071, *China*
[b)] *Graduate School of the Chinese Academy of Sciences, Bejing* 100049, *China*
[c)] *Department of Modern Physics, Lanzhou University, Lanzhou* 730000, *China*
[d)] *Department of Physics, National University of Singapore, 2 Science Drive 3,* 117542, *Singapore*

(Received 17 November 2008; revised manuscript received 3 December 2008)

We theoretically explore the possibility of realizing controllable thermal entanglement of effective spins in a four-qubit anisotropic Heisenberg XXZ coupling spin-star system constructed by coupled microcavities. We analyse the dependence of thermal entanglement in this system on temperature, inhomogeneity of the magnetic field, and anisotropy, which can be readily tuned via the external laser fields. The peculiar characteristic and the full controllability of the thermal entanglement are demonstrated to be useful for quantum information processing.

Keywords: thermal entanglement, Heisenberg model, cavity QED
PACC: 0365, 4250

1. Introduction

Quantum entanglement exhibits many distinctive features of many-body systems,[1] and the concept of thermal entanglement[2−7] is usually used to specify the amount of entanglement between two spins of a multi-spin system when the whole system is in thermal equilibrium. As a good measure of bipartite entanglement particularly suitable for spin one-half systems, concurrence[8] has been intensively investigated in various models.

On the other hand, much attention has been paid, over recent years, to characterizing qualitatively and quantitatively the entanglement properties of spin networks which would be useful for quantum information processing, such as the transfer of quantum states[9] and the generation of highly entangled states.[10] One of the most promising candidates for spin-qubit quantum computation is the spin-star network[11] due to its high symmetry, strong non-Markovian behaviour, and potential to scale up to larger systems. In such a spin-star system, the noncentral spins, called outer spins, interact exclusively and continuously with the central spin but not with each other. The exact quantum dynamics of one- and two-spin-qubit systems in a spin-star configuration has been derived and analysed by Heisenberg XY interaction,[12] and some protocols based on this system for quantum communication and for quantum cloning were proposed, such as the phase covariant cloning (PCC)[13] and universal quantum cloning.[14] In addition, the spin-star system has also been used for entanglement distribution[11,15] in a more effective way than other standard methods.

We have also noted that there are various ongoing efforts for the physical realization of an effective spin model by trapped ions,[16] quantum dots,[3,17] and cavity quantum electrodynamics (QED).[18−21] In Ref.[19], a novel scheme based on Λ level-structure atoms and cavity-mediated Raman transitions was designed to simulate an effective spin-1/2 interaction, and the complete effective Hamiltonian of the spin–spin interaction (i.e., the standard XXZ model) could be obtained via tunable experimental parameters, such as the atom–cavity coupling strength and

*Project supported by National Natural Science Foundation of China (Grant Nos 10774163, 10774042 and 10604025), and the National Fundamental Research Program of China (Grants Nos 2005CB724502 and 2006CB921203).
†Corresponding author. E-mail: mangfeng1968@yahoo.com

the Rabi frequencies relevant to the external laser fields. The system shows its great potential in the realization of quantum computation because of its good controllability and scalability. However, in any real situation, a maximally entangled state is difficult to prepare and maintain, and mixed states in thermal equilibrium as the resource are close to real circumstances. In this sense, the studies of thermal entanglement in the scheme and the evaluation of its controllability are valuable for further research in quantum information processing. Actually, we have noticed some recent work on applications of thermal entanglement, such as quantum teleportation[22] and gate operations for quantum computation.[23] So it would be interesting to explore the availability for practically engineering the thermal entanglement in a spin-star configuration based on the cavity–atom system. We want to show that this kind of effective spin system offers us a potential setting to enhance thermal entanglement and to analyse the dependence of entanglement on temperature and external magnetic field when the system remains in thermal equilibrium. We would also like to point out that using such an effective spin-star system to create and to increase spin thermal entanglement is feasible and flexible.

In what follows, we address the tunable thermal entanglement in a four-qubit anisotropic spin-star network with Heisenberg XXZ coupling, which could be constructed by atoms embedded in microcavities. We will explore the possibility of creating and tuning spin entanglement by controlling laser fields in the system. Our main concentration will be on the influence of temperature, non-uniform magnetic field, and the anisotropic parameter on the thermal entanglement between two of the spins. More importantly, we will demonstrate the tunability of entanglement under a certain maximal value in such a system with the help of external laser fields.

The remainder of the present paper is organized as follows. In Section 2 we outline the basic model in the effective spin-star system by using coupled microcavities. Then in Section 3, equations to evaluate the concurrence between an arbitrary pair of spins in this architecture will be analytically derived. In Section 4, we will discuss the influence of temperature, nonuniform magnetic field and the anisotropic parameter. The paper ends with a brief discussion and a summary in Section 5. Some details of our deductions are presented in an appendix.

2. The model

We sketch our idea with a spin-star configuration illustrated in Fig.1, which consists of $N+1$ atoms localized separately in $N+1$ microcavities coupled via exchange of photons with one Λ-type atom in each microcavity. One of the microcavities is located at site 0 (i.e. the centre of the configuration), while the other microcavities (labelled by index $i = 1, 2, ..., N$) are located on a circle surrounding the central spin with equal distance in between them. We employ the long-lived levels $|0\rangle$ and $|1\rangle$ as $|-1/2\rangle$ and $|1/2\rangle$ spin states, respectively, and the cavity modes couple with strengths g_0 and g_1 to the transitions $|0\rangle \leftrightarrow |e\rangle$ and $|1\rangle \leftrightarrow |e\rangle$, respectively. As depicted in Ref.[19], single atoms in interacting cavities that are operated in strong coupling regimes can form a spin-1/2 effective Hamiltonian. To produce a complete effective XYZ model for each atom, one should turn on the lasers to generate the XY-type coupling for a short time interval $\mathrm{d}t$ followed by another time interval $\mathrm{d}t'$ with the lasers generating the ZZ-type coupling (see Figs.2(a) and 2(b)). The radiation sequences under the requirements $||H_{xy}|| \cdot \mathrm{d}t \ll 1$ and $||H_{zz}|| \cdot \mathrm{d}t' \ll 1$ should be repeated until the effective XYZ model is achieved.

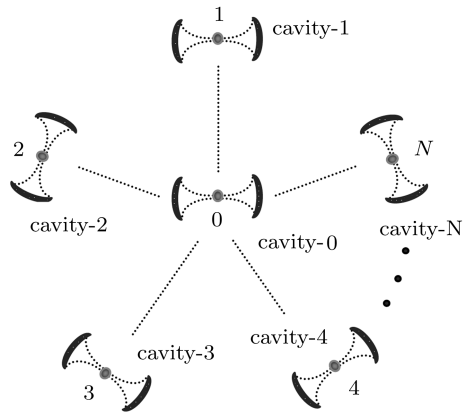


Fig.1. A schematic diagram for the spin-star configuration via coupled microcavities connected by optical fibres. The atom labelled with 0 has a central spin, which interacts with all other $(1-N)$ spins surrounding it.

For simplicity, in the following we will focus exclusively on the case of the four-qubit anisotropic Heisenberg XXZ model in this spin-star configuration. In fact, as inhomogeneity of the magnetic field is inevitable in a real system, it is necessary to consider the effect of a nonuniform magnetic field in this XXZ-type coupling system. Here we only consider the following simple case: except the central spin, all the

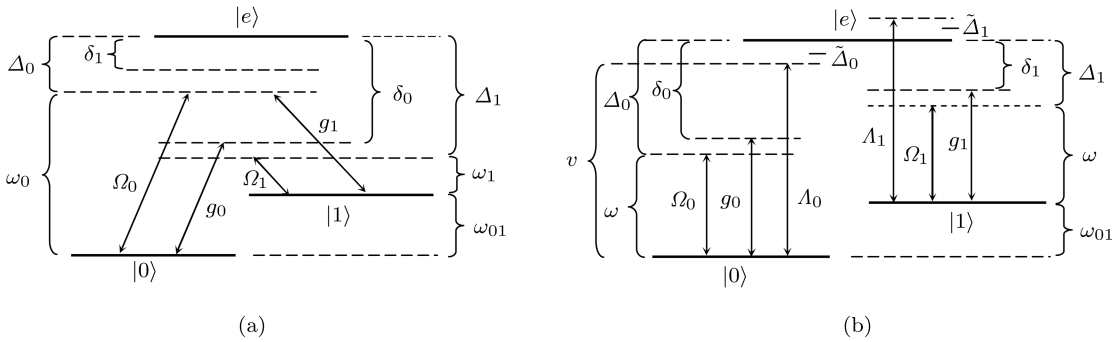


Fig.2. Atomic level structure with driving lasers and relevant couplings to the cavity mode, which, cited from Ref.[18], are replotted for the convenience of our description in the text. (a) The generation of effective Heisenberg XY-couplings for one atom, where one should irradiate each atom by using one laser with Rabi frequency Ω_0, coupled to the transtion $|0\rangle \leftrightarrow |e\rangle$ with frequency ω_0 and another laser with Rabi frequency Ω_1, coupled to the transtion $|1\rangle \leftrightarrow |e\rangle$ with frequency ω_1, where $\delta_1 = \omega_{01} - (\omega_0 - \omega_1)/2$, $\Delta_0 \equiv \omega_e - \omega_0$, and $\Delta_1 \equiv \omega_e - (\omega_0 + \omega_1)/2$. (b) The generation of effective Heisenberg ZZ-couplings for one atom, where one should irradiate each atom by using one pair of lasers with Rabi frequency Ω_0 and Λ_0, coupled to the transtion $|0\rangle \leftrightarrow |e\rangle$ with frequency ω, υ, respectively, and another pair of lasers with Rabi frequency Ω_1 and Λ_1, coupled to the transtion $|1\rangle \leftrightarrow |e\rangle$ with frequency ω, υ, respectively, where $\Delta_0 \equiv \omega_e - \omega$, $\Delta_1 \equiv \omega_e - \omega - \omega_{01}$, $\tilde{\Delta}_0 \equiv \omega_e - \upsilon$ and $\tilde{\Delta}_1 \equiv \omega_e - \upsilon - \omega_{01}$.

other outer spins are under a uniform external magnetic field B_1. From the discussion above, the corresponding Hamiltonian could be given as below,

$$H_s = \sum_{j=1}^{3}(J\sigma_0^x\sigma_j^x + J\sigma_0^y\sigma_j^y + \lambda\sigma_0^z\sigma_j^z + B_1\sigma_j^z) + B_0\sigma_0^z, \quad (1)$$

where the exchange coupling coefficient in the x-y plane is represented by[24]

$$J = \frac{\beta_1 |\Omega_1|^2 g_0^2}{8\Delta_1^2}, \quad (2)$$

where we present $J = J_x = J_y = \dfrac{\beta_1 |\Omega_1|^2 g_0^2}{8\Delta_1^2}$ by setting $\Omega_0 \to 0$ from the model in Ref.[19] with $\beta_1 = \dfrac{1}{4}\sum_k \frac{1}{(\omega_0+\omega_1)/2-\omega_k}$, and $\Delta_1 \equiv \omega_e - (\omega_0 + \omega_1)/2$. The parameters in the above two equations are labelled in Fig.2(a) with the same definitions as in Ref.[19]. But as we only consider XXZ coupling, we have simply assumed in expression (2) and thereafter one of the lasers with negligibly small coupling to the atom in each cavity.[19] Similarly, the anisotropy is defined as,

$$\lambda = \beta_2 \left| \frac{\Omega_1^* g_1}{4\Delta_1} - \frac{\Omega_0^* g_0}{4\Delta_0} \right|^2 \quad (3)$$

with $\beta_2 = \dfrac{1}{4}\sum_k \dfrac{1}{\omega - \omega_k}$, $\Delta_0 = \omega_e - \omega$, and $\Delta_1 = \omega_e - \omega - \omega_{01}$. Note that the anisotropic term is added by an additional physical process.[19] So like Ref.[19], we use the same symbols, e.g. Ω_1 and Δ_1, with different values in expressions (2) and (3) for different processes. For $\lambda = J$ and $\lambda = 0$, we call expression (l) XXX and XX models, respectively. In other words, the XX and XXX models can be regarded as special cases of the XXZ model. For the convenience of the following study, we will work in energy units of $J = 1$ so that B_0, B_1, and λ are dimensionless, where

$B_0 = \tilde{B} + \tilde{B}'$, and $\tilde{B} = \delta_1/2 - \dfrac{1}{2}\left[\dfrac{|\Omega_1|^2}{4\Delta_1^2}\left(\Delta_1 - \dfrac{|\Omega_1|^2}{4\Delta_1} - \gamma_1 g_1^2 - \beta_3 g_0^2 + \beta_3^2 \dfrac{g_0^4}{\Delta_1}\right)\right]$, and $\tilde{B}' = \dfrac{1}{2}\left[\dfrac{|\Lambda_1|^2}{16\tilde{\Delta}_1^2}\left(4\tilde{\Delta}_1 - \dfrac{|\Lambda_0|^2}{\tilde{\Delta}_0 - \tilde{\Delta}_1} - \dfrac{|\Lambda_1|^2}{\tilde{\Delta}_1} - \sum_{j=0,1}\left(\dfrac{|\Omega_j|^2}{\Delta_j - \tilde{\Delta}_1} + 4\tilde{\gamma}_{j1} g_j^2\right) + \dfrac{|\Omega_1|^2}{16\Delta_1^2}\left(4\Delta_1 - \dfrac{|\Omega_0|^2}{\Delta_0 - \Delta_1} - \dfrac{|\Omega_1|^2}{\Delta_1} - \sum_{j=0,1}\left(4\gamma_{j1} g_j^2 + \dfrac{|\Lambda_j|^2}{\tilde{\Delta}_j - \Delta_1}\right)\right.\right.\right.$
$\left.\left.\left. + 4\gamma_{11}^2 \dfrac{g_1^4}{\Delta_1}\right) - (0 \leftrightarrow 1)\right]$ with $\delta_1 = \omega_{01} - (\omega_0 - \omega_1)/2$, $\gamma_1 = \dfrac{1}{4}\sum_k \dfrac{1}{\omega_{0,1} - \omega_k}$, $\beta_3 = \dfrac{1}{4}\sum_k \dfrac{1}{(\omega_0 + \omega_1)/2 - \omega_k}$,
$\gamma_{00} = \gamma_{11} = \dfrac{1}{4}\sum_k \dfrac{1}{\omega - \omega_k}$, $\gamma_{01} = \dfrac{1}{4}\sum_k \dfrac{1}{\omega + \omega_{01} - \omega_k}$, $\gamma_{10} = \dfrac{1}{4}\sum_k \dfrac{1}{\omega - \omega_{01} - \omega_k}$, $\tilde{\gamma}_{01} = \dfrac{1}{4}\sum_k \dfrac{1}{\upsilon + \omega_{01} - \omega_k}$,
$\tilde{\gamma}_{10} = \dfrac{1}{4}\sum_k \dfrac{1}{\upsilon - \omega_{01} - \omega_k}$, $\tilde{\gamma}_{00} = \tilde{\gamma}_{11} = \dfrac{1}{4}\sum_k \dfrac{1}{\upsilon - \omega_k}$, $\tilde{\Delta}_0 \equiv \omega_e - \upsilon$, $\tilde{\Delta}_1 \equiv \omega_e - \upsilon - \omega_{01}$.

Note that B_1, with the same definition as B_0, could be of identical or different values from B_0. But B_0 is related to the central microcavity (or spin), whereas B_1 is in charge of the outer ones. It is clear from the above relations that the effective magnetic field $\tilde{B}$ and $\tilde{B}'$ could be tuned independently to any values by varying Ω_0, Ω_1, Λ_0 and Λ_1. In the present scheme, J and λ could be tuned to all required values by controlling the parameters in a straightforward way. In addition, the discrepancies between B_0 and B_1, reflecting the inhomogeneity of the magnetic field, could also be tuned to any advisable values by suitably varying the parameters such as Ω_0, Ω_1, Λ_0, and Λ_1. As the physics of expression (1) regarding the coupled microcavities has been discussed in detail in Ref.[19], we will mainly pay attention to expression (1) itself below.

3. Thermal entanglement

A straightforward calculation gives eigenvalues of the Hamiltonian in expression (1),

$$\begin{aligned}
&E_{1,2} = \lambda + B_+, \;\; E_{3,4} = \lambda - B_+, \\
&E_{5,6} = -\lambda + \sqrt{P}, \;\; E_{7,8} = -\lambda - \sqrt{P}, \\
&E_{9,10} = -\lambda - 2B_1 \pm \sqrt{D + 4\lambda(\lambda - B_-)}, \\
&E_{11,12} = 3\lambda \pm (B_0 + 3B_1), \\
&E_{13,14} = -\lambda + 2B_1 \pm \sqrt{D + 4\lambda(\lambda + B_-)}, \\
&E_{15,16} = -\lambda \pm \sqrt{Q}, \qquad (4)
\end{aligned}$$

where $B_\pm = B_0 \pm B_1$, $P = B_-^2 + 4J^2$, $D = B_-^2 + 12J^2$, and $Q = B_-^2 + 16J^2$, and we take $J = 1$ throughout the calculation in this work. The corresponding eigenstates can be explicitly denoted as

$$\begin{aligned}
&|\Psi\rangle_1 = \frac{1}{\sqrt{2}}(|0010\rangle - |0001\rangle), \;\; |\Psi\rangle_2 = \frac{1}{\sqrt{2}}(|0100\rangle - |0001\rangle), \\
&|\Psi\rangle_3 = \frac{1}{\sqrt{2}}(|1101\rangle - |1011\rangle), \;\; |\Psi\rangle_4 = \frac{1}{\sqrt{2}}(|1110\rangle - |1011\rangle), \\
&|\Psi\rangle_5 = N_5 \left(|0101\rangle - |0011\rangle + \frac{B_- - \sqrt{P}}{2J} |1010\rangle + \frac{-B_- + \sqrt{P}}{2J} |1100\rangle \right), \\
&|\Psi\rangle_6 = N_6 \left(|1001\rangle - |1100\rangle + \frac{B_- + \sqrt{P}}{2J} |0011\rangle + \frac{-B_- - \sqrt{P}}{2J} |0110\rangle \right), \\
&|\Psi\rangle_7 = N_7 \left(|0101\rangle - |0011\rangle + \frac{B_- + \sqrt{P}}{2J} |1010\rangle - \frac{B_- + \sqrt{P}}{2J} |1100\rangle \right), \\
&|\Psi\rangle_8 = N_8 \left(|1001\rangle - |1100\rangle + \frac{B_- - \sqrt{P}}{2J} |0011\rangle + \frac{-B_- + \sqrt{P}}{2J} |0110\rangle \right), \\
&|\Psi\rangle_{9,10} = N_{9,10} \left(|1011\rangle + |1101\rangle + |1110\rangle + \frac{B_- - 2\lambda \pm \sqrt{D + 4\lambda(\lambda - B_-)}}{2J} |0111\rangle \right), \\
&|\Psi\rangle_{11} = |0000\rangle, \qquad |\Psi\rangle_{12} = |1111\rangle, \\
&|\Psi\rangle_{13,14} = N_{13,14} \left(|0001\rangle + |0010\rangle + |0100\rangle + \frac{-B_- - 2\lambda \pm \sqrt{D + 4\lambda(\lambda + B_-)}}{2J} |0111\rangle \right), \\
&|\Psi\rangle_{15,16} = N_{15,16} \left[\frac{-B_- \pm \sqrt{Q}}{4J} (|1001\rangle + |1010\rangle + |1100\rangle) + |0011\rangle + |0101\rangle + |0110\rangle \right], \qquad (5)
\end{aligned}$$

with N_i $(i = 5, 6, \ldots)$ being normalization constants.

We consider below that thermal fluctuation is involved in the system. The system in thermal equilibrium with temperature T could be characterized by a density operator $\rho(T) = (1/Z)\exp(-\beta H_{\rm s})$, where $\beta = 1/k_{\rm B}T$ with $k_{\rm B}$ being the Boltzmann constant and $Z = {\rm Tr}\{\exp(-\beta H_{\rm s})\}$ the partition function. For the convenience of calculation, we will set $k_{\rm B} = 1$, and thereby T is in units of energy (a conversion to units of kelvins could be made by division by $k_{\rm B}$) and can be described dimensionlessly like B_0, B_1, and λ. The entanglement of this density matrix $\rho(T)$ is called the thermal entanglement of the spin system. As a measure of thermal entanglement in most previous investigations, the concurrence[8,27] of two qubits is calculated from the following relation:

$$C_{\rm AB} = \max\left\{ \left[\sqrt{\xi_1} - \sum_{i=2}^{4} \sqrt{\xi_i} \right]; 0 \right\}, \qquad (6)$$

where the values arranged in a descending order $\{\xi_1,\ \xi_2,\ \xi_3,\ \xi_4\}$ are four non-negative eigenvalues of the joint density matrix $\varrho = \rho_{AB}(\sigma_A^y \otimes \sigma_B^y)\rho_{AB}^*(\sigma_A^y \otimes \sigma_B^y)$, with ρ_{AB} being the density matrix of the system consisting of qubits A and B, and the asterisk denotes the complex conjugate. As the spin-star configuration with couplings of equal strength has symmetric properties due to its invariance under the exchange of any outer spin, we have in this four-qubit spin-star system,

$$\begin{aligned} C_{01} &= C_{02} = C_{03}, \\ C_{12} &= C_{23} = C_{13}. \end{aligned} \tag{7}$$

The trace-over for obtaining a reduced density matrix is done in the subspace spanned by the eigenstates in expression (5). We take the concurrence C_{01} and C_{23} as examples below. In the standard bases $\{|00\rangle, |01\rangle, |10\rangle, |11\rangle\}$, the reduced density matrixes $\rho_{01}(T)$ and $\rho_{23}(T)$ can be written as

$$\rho_{01}(T) = \frac{1}{Z}\begin{pmatrix} u_{01} & 0 & 0 & 0 \\ 0 & w_{01} & y_{01} & 0 \\ 0 & y_{01} & w_{01} & 0 \\ 0 & 0 & 0 & v_{01} \end{pmatrix}, \tag{8}$$

and

$$\rho_{23}(T) = \frac{1}{Z}\begin{pmatrix} u_{23} & 0 & 0 & 0 \\ 0 & w_{23} & y_{23} & 0 \\ 0 & y_{23} & w_{23} & 0 \\ 0 & 0 & 0 & v_{23} \end{pmatrix}.$$

Based on the definition of concurrence, we can obtain the analytical expressions of C_{01} and C_{23} at a finite temperature.

$$\begin{aligned} C_{01}(T) &= \frac{2}{Z}\max\{|y_{01}| - \sqrt{u_{01}v_{01}}, 0\}, \\ C_{23}(T) &= \frac{2}{Z}\max\{|y_{23}| - \sqrt{u_{23}v_{23}}, 0\}. \end{aligned} \tag{9}$$

Detailed analytical formulas are presented in the Appendix.

4. Influence from temperature, non-uniform field and anisotropy

To present the specific variation of entanglement in the system, we have made some numerical calculations. In Fig.3, we mainly concentrate on the effect of temperature on the concurrences C_{01} and C_{23} under different magnetic fields when the anisotropy parameter takes a fixed value of 0.5. We may find that under the same situation, the concurrence C_{01} is generally larger than C_{23}, which is due to the fact that there exists direct spin-spin coupling between the central spin and each outer spin, but correlation among the outer spins is only achieved via the central spin. However, this characteristic seems untrue when B_0 is much bigger than B_1, e.g. $B_1 = B_0/10$, where C_{23} could reach a considerably big value of 0.52 at $T = 0.1$ and $|B_0| = 8$. It, on the one hand, demonstrates the important role that B_0 plays, and, on the other hand, reminds us of the availability of making the external magnetic field a favourable factor for thermal entanglement. In view of quantum networks, a highly desired goal would be the capability to produce and manipulate a large amount of entanglement between distant subsystems. It is evident that some big values of B_0 could significantly enchance the mediating capability of the central spin and lead C_{23} to be even larger than C_{01}. This impression of the strong role that B_0 plays could be strengthened when we consider the two magnetic fields in parallel or in anti-parallel. As depicted in the bottom plots of Fig.3, the flip of one of the magnetic fields, in the case of $B_0 \gg B_1$, leads to a significant change of concurrence, whereas it has almost no influence on concurrence in the case of $B_0 \ll B_1$. Moreover, temperature generally exhibits a destructive impact on thermal entanglement, while if $|B_0| \ll |B_1|$, the influence from temperature seems negligible.

In the case of two identically directed magnetic fields with $B_1 = B_0$, there are plateaus in C_{01} and C_{23} at $T = 0.1$ with $C_{01} = 0.555$ and $C_{23} = 0.241$, and all the plateaus in C_{01} and C_{23} fall off sharply at a certain magnetic field $|B_0| = 2.50$. Mathematically, the low temperature could lead to significant variation of the matrix elements and the partition function as shown in equations in the appendix. Physically, it could be understood that at lower temperatures the entanglement is more sensitive to the variation of external magnetic field. For this property, a possible usage is expected, for example, to make an effective switch to turn entanglement on or off by changing the external magnetic field.

To clarify, we also calculate some cases of $B_1 \neq B_0$ and $\lambda \neq 0.5$ as shown in Fig.4, from which we know that the plateaus strongly depend on the homogeneity of the magnetic field. A tiny inhomogeneity could lead the top of the plateaus to be slanted, whereas the anisotropic parameter only changes the width of the plateaus.

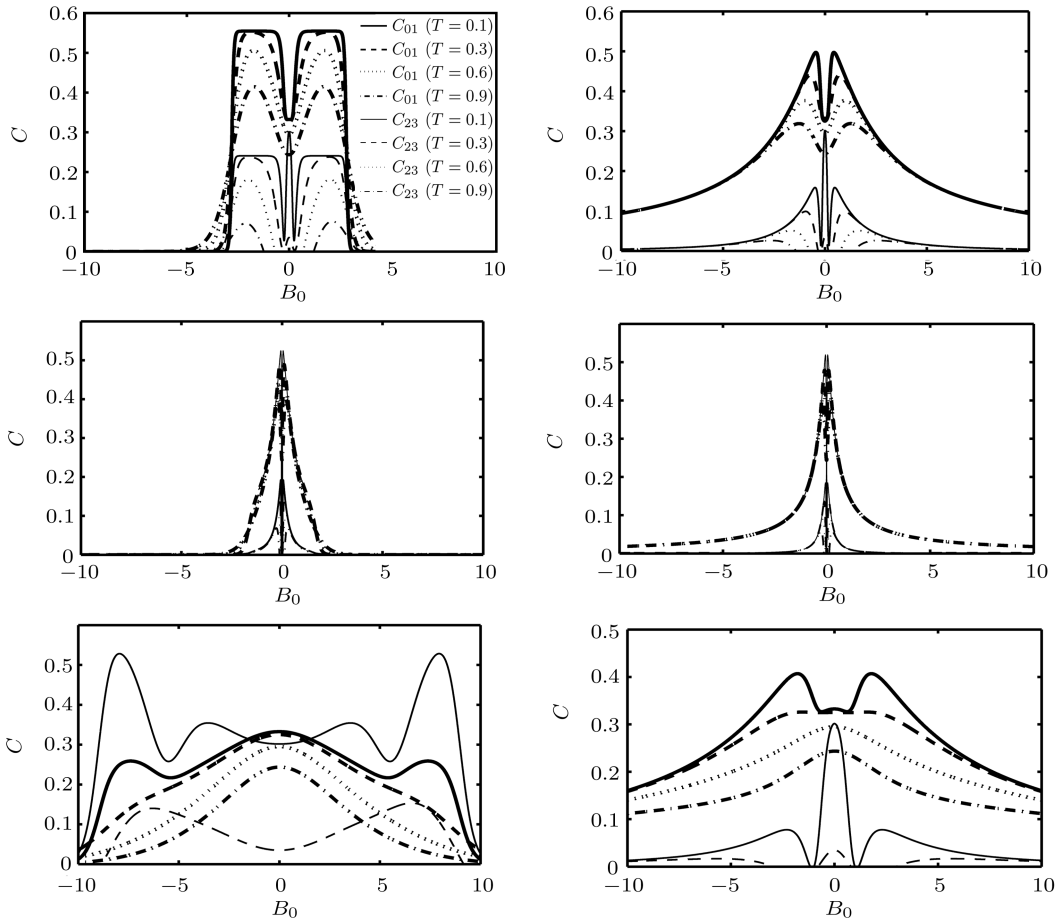


Fig.3. Concurrences C_{01} and C_{23} versus magnetic field B_0 at different temperatures and $\lambda = 0.5$.

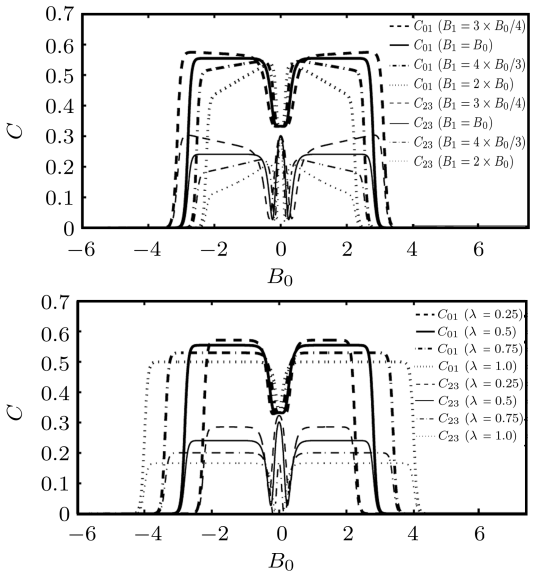


Fig.4. Concurrences C_{01} and C_{23} versus magnetic field B_0 at $T = 0.1$, where the top panel is for different values of B_0 and B_1 ($B_0 \neq B_1$) and the bottom panel is for different values of λ.

We have plotted Figs.5 and 6 to show the effect of the anisotropic parameter λ, from which we could find the maximum concurrence obtainable by changing λ. For the purpose of quantum networks, here we focus only on the critical point $\lambda^{\rm c}$, at which entanglement attains maximal values. To be clear, we list some values in Table 1 for the case of $B_0 = B_1$, from which we see that the critical anisotropic parameters $\lambda_{01}^{\rm c}$ and $\lambda_{23}^{\rm c}$ increase with B_0, but $C_{01}^{\max}$ and $C_{23}^{\max}$ decrease with B_0 if $B_0 \geq 3$. As parameters λ and J can be controlled separately, we are able to enhance the entanglement at our will by tuning the parameters in a coupled microcavity system at a sufficiently low temperature.

The characteristic above shows the star-shape configuration with cavity–atom subsystems to be a good candidate for quantum networks, because we can obtain thermal entanglement by controlling the parameters. For instance, to obtain an optimal concurrence, we could tune the magnetic fields by varying the external parameters of the laser fields in the coupled microcavities, such as Ω_0, Ω_1, Λ_0, and Λ_1.[25]

Table 1. Values of λ_{01}^{c} and λ_{23}^{c} in the case of $B_0 = B_1$.

B_0	$B_0 = 1$	$B_0 = 2$	$B_0 = 3$	$B_0 = 4$	$B_0 = 5$	$B_0 = 6$	$B_0 = 7$	$B_0 = 8$
λ_{01}^{c}	0.439	0.595	0.970	1.351	1.727	2.095	2.460	2.818
C_{01}^{max}	0.477	0.526	0.490	0.443	0.398	0.358	0.325	0.296
λ_{23}^{c}	0	0.435	0.857	1.256	1.641	2.016	2.383	2.750
C_{23}^{max}	0.178	0.211	0.167	0.127	0.097	0.076	0.060	0.049

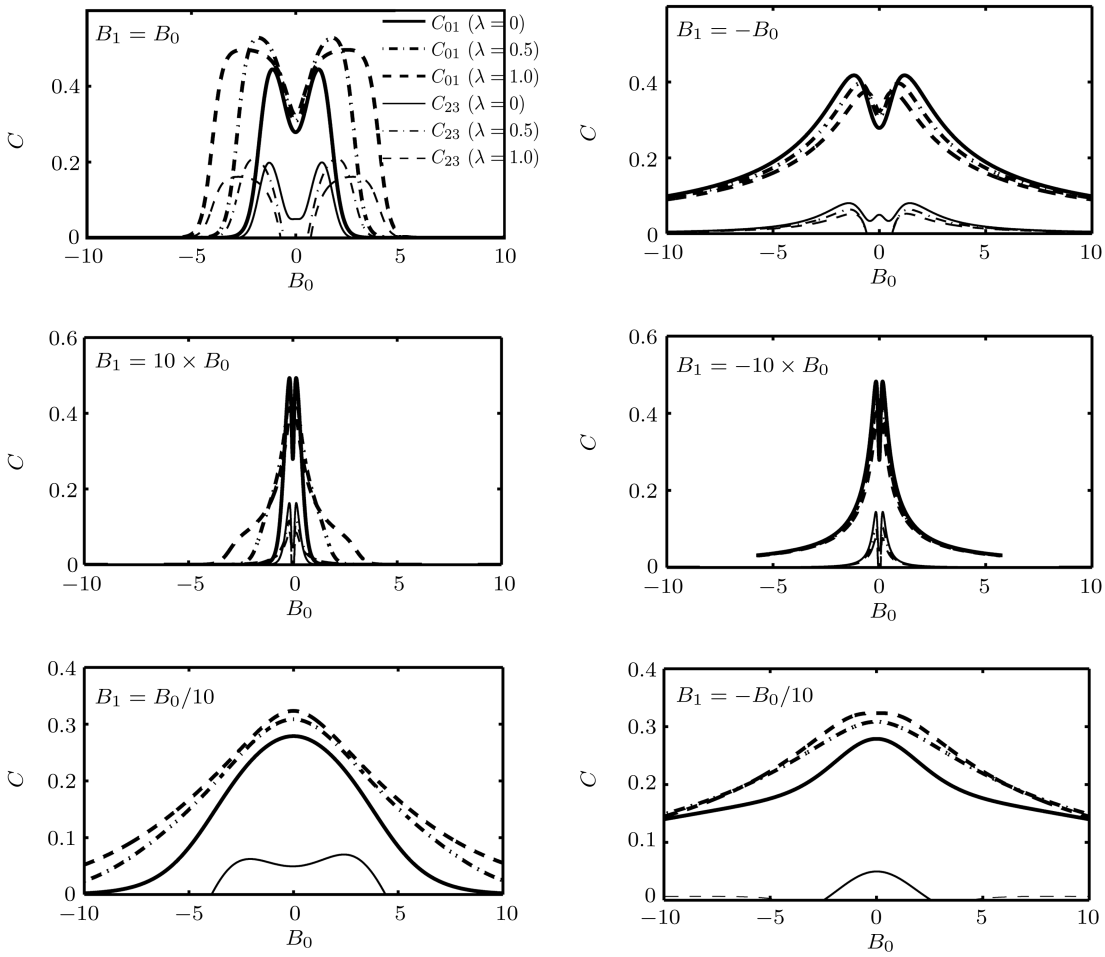
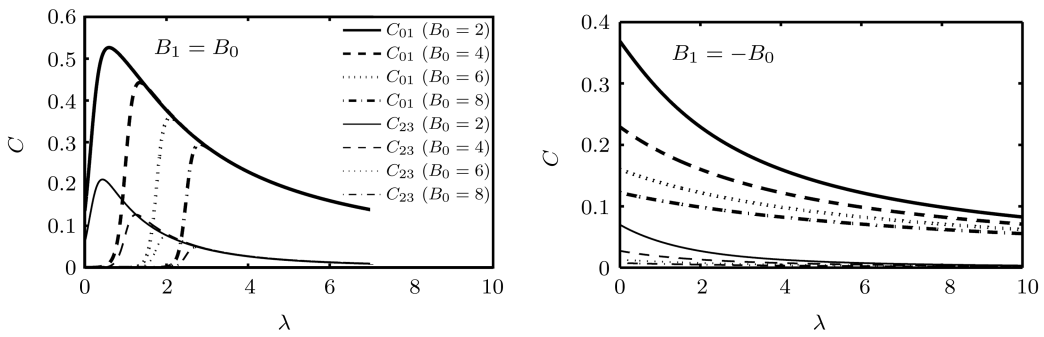


Fig.5. Concurrences C_{01} and C_{23} versus magnetic field B_0 at different values of parameter λ and $T = 0.5$.



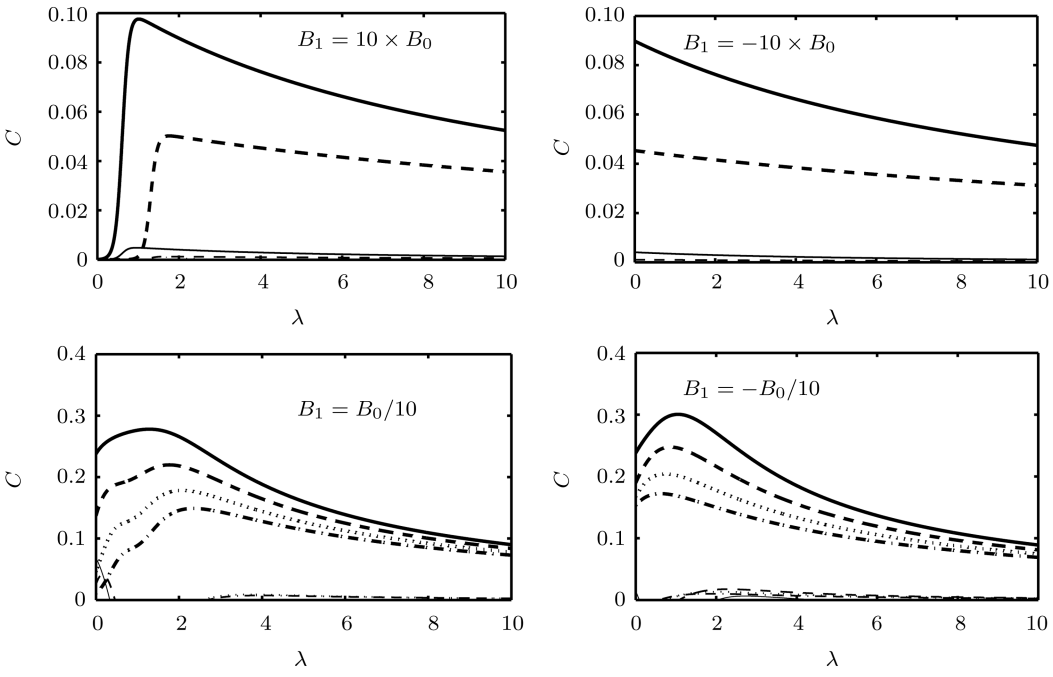


Fig.6. Concurrences C_{01} and C_{23} versus anisotropic parameter λ under different magnetic fields and at $T = 0.5$.

5. Discussion and conclusion

All the results above not only provide us with useful information about the tunable thermal entanglement depending on various system parameters, but are also conducive to the investigation of entanglement production and manipulation in other spin-qubit models. The pairwise entanglement in our system at thermal equilibrium exhibits some interesting phenomena, depending on temperature, inhomogeneity of the magnetic field and anisotropy. Based on these properties, we may have our desired entanglement by tuning the parameters relevant to the microcavity system, particularly by changing the intensities and the frequencies of the lasers. Due to the full controllability of the parameters, we might consider a more complicated spin-star configuration for doing jobs in quantum networks, such as the transfer of quantum state and the distribution of entanglement,[11] as well as the implementation of one-way quantum computing.[10] These explorations will be carried out in our future work.

As in Ref.[19], in the present paper we consider a strong coupling regime in high-Q microcavities connected by lossless fibres, which allows us to omit decoherence in our treatment. This is also the advantage of this kind of effective spin system over the real spin system under strong correlation in magnetic compounds. Besides, the spatial separation of the microcavities makes it possible to individually manipulate the spins, which is an essential prerequisite for quantum information processing. Moreover, what we have investigated is the case of XXZ coupling. Actually, the effective spin system of coupled microcavities could yield a XYZ-type model, which is more complicated in treatment and analysis but would allow larger ranges of values for the parameters to vary. So we would hopefully find more practical potential in such effective systems for quantum information processing.

In summary, we have theoretically studied the possibility of optimizing spin entanglement in a thermal system with coupled microcavities by changing relevant parameters. We have given exact analytical solutions of the concurrence between any two of the qubits. We have demonstrated the dependence of the entanglement on temperature, inhomogeneity of magnetic field, and anisotropy. Our work shows that a fully controllable entanglement between spins under thermal equilibrium is feasible with cavity QED technology, which would be used for quantum information tasks. We would also like to point out that the scenario considered in this work is relatively simple but physically fundamental. So the results we presented above could be directly applied

to more complicated cases, such as more outer spins. If different magnetic fields on the outer spins and more couplings in the star configuration are involved, however, there would be a more complicated variation in the concurrence. Nevertheless, it would be of more practical importance and a more attractive proposition to extend such a model to more realistic scenarios and more qubits, which are under consideration.

Appendix

For completeness we present the following complete analytical expressions relevant to the elements of reduced density matrixes $\rho_{01}(T)$ and $\rho_{23}(T)$. The corresponding matrix elements and the partition function have the following forms:

$$\begin{aligned} u_{01} = {} & \frac{3}{2}\exp\left(\frac{-\lambda - B_+}{T}\right) + \exp\left(\frac{-3\lambda - B_0 - 3B_1}{T}\right) + \exp\left(\frac{\lambda}{T}\right)\left[\frac{1}{3}\cosh\left(\frac{\sqrt{Q}}{T}\right) - \frac{B_-}{3\sqrt{Q}}\sin\left(\frac{\sqrt{Q}}{T}\right)\right] \\ & + \exp\left(\frac{\lambda}{T}\right)\left[\cosh\left(\frac{\sqrt{P}}{T}\right) - \frac{B_-}{\sqrt{P}}\sin\left(\frac{\sqrt{P}}{T}\right)\right] \\ & + 8J^2 \times \exp\left(\frac{\lambda - 2B_1}{T}\right) \times \left[\frac{\exp\left(\frac{-\Theta_+}{T}\right)}{12J^2 + \Gamma_2^2} + \frac{\exp\left(\frac{\Theta_+}{T}\right)}{12J^2 + \Gamma_1^2}\right], \end{aligned} \tag{A1}$$

$$\begin{aligned} v_{01} = {} & \exp\left(\frac{-\lambda + B_+}{T}\right) + \exp\left(\frac{-3\lambda + B_0 + 3B_1}{T}\right) + \exp\left(\frac{\lambda}{T}\right)\left[\frac{1}{3}\cosh\left(\frac{\sqrt{Q}}{T}\right) + \frac{B_-}{3\sqrt{Q}}\sin\left(\frac{\sqrt{Q}}{T}\right)\right] \\ & + \exp\left(\frac{\lambda}{T}\right)\left[\cosh\left(\frac{\sqrt{P}}{T}\right) + \frac{B_-}{\sqrt{P}}\sin\left(\frac{\sqrt{P}}{T}\right)\right] \\ & + 8J^2 \times \exp\left(\frac{\lambda + 2B_1}{T}\right) \times \left[\frac{\exp\left(\frac{-\Theta_-}{T}\right)}{12J^2 + \Gamma_3^2} + \frac{\exp\left(\frac{\Theta_-}{T}\right)}{12J^2 + \Gamma_4^2}\right], \end{aligned} \tag{A2}$$

$$\begin{aligned} y_{01} = {} & 2J \times \exp\left(\frac{\lambda + 2B_1}{T}\right)\left[\frac{\Gamma_3 \exp\left(\frac{-\Theta_-}{T}\right)}{12J^2 + \Gamma_3^2} + \frac{\Gamma_4 \exp\left(\frac{\Theta_-}{T}\right)}{12J^2 + \Gamma_4^2}\right] \\ & + 2J \times \exp\left(\frac{\lambda - 2B_1}{T}\right)\left[\frac{\Gamma_2 \exp\left(\frac{-\Theta_+}{T}\right)}{12J^2 + \Gamma_2^2} - \frac{\Gamma_1 \exp\left(\frac{\Theta_+}{T}\right)}{12J^2 + \Gamma_1^2}\right] - \frac{2\sqrt{Q - B_-^2}}{3\sqrt{Q}}\exp\left(\frac{\lambda}{T}\right)\sinh\left(\frac{\sqrt{Q}}{T}\right), \end{aligned} \tag{A3}$$

$$\begin{aligned} u_{23} = {} & \frac{1}{2}\exp\left(\frac{-\lambda - B_+}{T}\right) + \exp\left(\frac{-3\lambda - B_0 - 3B_1}{T}\right) + \exp\left(\frac{\lambda}{T}\right)\left[\frac{1}{3}\cosh\left(\frac{\sqrt{Q}}{T}\right) + \frac{B_-}{3\sqrt{Q}}\sin\left(\frac{\sqrt{Q}}{T}\right)\right] \\ & + \exp\left(\frac{\lambda}{T}\right) \times \left[\cosh\left(\frac{\sqrt{P}}{T}\right) + \frac{B_-}{\sqrt{P}}\sin\left(\frac{\sqrt{P}}{T}\right)\right] + \exp\left(\frac{\lambda - 2B_1}{T}\right) \\ & \times \left\{\frac{[4J^2 + \Gamma_2^2]\exp\left(\frac{-\Theta_+}{T}\right)}{12J^2 + \Gamma_2^2} + \frac{[4J^2 + \Gamma_1^2]\exp\left(\frac{\Theta_+}{T}\right)}{12J^2 + \Gamma_1^2}\right\}, \end{aligned} \tag{A4}$$

$$\begin{aligned} v_{23} = {} & \exp\left(\frac{-\lambda + B_+}{T}\right) + \exp\left(\frac{-3\lambda + B_0 + 3B_1}{T}\right) + \exp\left(\frac{\lambda}{T}\right)\left[\frac{1}{3}\cosh\left(\frac{\sqrt{Q}}{T}\right) - \frac{B_-}{3\sqrt{Q}}\sin\left(\frac{\sqrt{Q}}{T}\right)\right] \\ & + \exp\left(\frac{\lambda}{T}\right) \times \left[\cosh\left(\frac{\sqrt{P}}{T}\right) - \frac{B_-}{\sqrt{P}}\sin\left(\frac{\sqrt{P}}{T}\right)\right] + \exp\left(\frac{\lambda + 2B_1}{T}\right) \end{aligned}$$

$$\times \left\{ \frac{[4J^2+\Gamma_3^2]\exp\left(\dfrac{-\Theta_-}{T}\right)}{12J^2+\Gamma_3^2} + \frac{[4J^2+\Gamma_4^2]\exp\left(\dfrac{\Theta_-}{T}\right)}{12J^2+\Gamma_4^2} \right\}, \tag{A5}$$

$$y_{23} = -\frac{1}{2}\exp\left(\frac{-\lambda-B_+}{T}\right) + 4J^2 \times \exp\left(\frac{\lambda+2B_1}{T}\right)\left[\frac{\exp\left(\dfrac{-\Theta_-}{T}\right)}{12J^2+\Gamma_3^2} + \frac{\exp\left(\dfrac{\Theta_-}{T}\right)}{12J^2+\Gamma_4^2}\right] + \frac{2}{3}\exp\left(\frac{\lambda}{T}\right)\cosh\left(\frac{\sqrt{Q}}{T}\right)$$
$$+\ 4J^2 \times \exp\left(\frac{\lambda-2B_1}{T}\right) \times \left[\frac{\exp\left(\dfrac{-\Theta_+}{T}\right)}{12J^2+\Gamma_2^2} + \frac{\exp\left(\dfrac{\Theta_+}{T}\right)}{12J^2+\Gamma_1^2}\right], \tag{A6}$$

$$\begin{aligned} Z =& 4\exp\left(-\frac{\lambda}{T}\right)\cosh\left(\frac{B_+}{T}\right) + 4\exp\left(\frac{\lambda}{T}\right)\cosh\left(\frac{\sqrt{P}}{T}\right) + 2\exp\left(\frac{\lambda}{T}\right)\cosh\left(\frac{\sqrt{Q}}{T}\right) \\ &+ 2\exp\left(-\frac{3\lambda}{T}\right)\cosh\left(\frac{B_0+3B_1}{T}\right) + 2\exp\left(\frac{\lambda-2B_1}{T}\right)\cosh\left(\frac{\Theta_+}{T}\right) \\ &+ 2\exp\left(\frac{\lambda+2B_1}{T}\right)\cosh\left(\frac{\Theta_-}{T}\right), \end{aligned} \tag{A7}$$

where

$$\begin{aligned} &\Theta_\pm = \sqrt{D+4\lambda(\lambda\pm B_-)}, \quad \Gamma_1 = \Theta_+ + B_- + 2\lambda, \\ &\Gamma_2 = \Theta_+ - B_- - 2\lambda, \quad \Gamma_3 = \Theta_- + B_- - 2\lambda, \quad \Gamma_4 = \Theta_- - B_- + 2\lambda. \end{aligned} \tag{A8}$$

References

[1] Nielsen M A and Chuang I L 2001 *Quantum Computation and Quantum Information* (Cambridge: Cambridge University Press)

[2] Vala J and Whaley B 2002 *Phys. Rev.* A **66** 022304

[3] Burkard G, Loss D and Divincenzo D P 1999 *Phys. Rev.* B **59** 2070

[4] Hill S and Wootters W K 1997 *Phys. Rev. Lett.* **78** 5022

[5] Amico L, Osterloh A, Plastina F, Fazio R and Palma M 2004 *Phys. Rev.* A **69** 022304

[6] Osterloh A, Amico L, Falci G and Fazio R 2002 *Nature* **416** 608

[7] Zhou L, Yi X X, Song H S and Guo Y Q 2005 *Chin. Phys.* **14** 1168
Qin M, Xu S L, Tao Y G and Tian D P 2008 *Chin. Phys.* B **17** 2800
Huang L Y and Fang M F 2008 *Chin. Phys.* B **17** 2339

[8] Wootters W K 1998 *Phys. Rev. Lett.* **80** 2245

[9] Christandl M, Datta N, Ekert A and Landahl A J 2004 *Phys. Rev. Lett.* **92** 187902
Albanese C, Christandl M, Datta N and Ekert A 2004 *Phys. Rev. Lett.* **93** 230502
Yung M H and Bose S 2005 *Phys. Rev.* A **71** 032310

[10] Raussendorf R and Briegel H J 2001 *Phys. Rev. Lett.* **86** 5188
Gross D and Eisert J 2007 *Phys. Rev. Lett.* **98** 220503

[11] Hutton A and Bose S 2004 *Phys. Rev.* A **69** 042312

[12] Breuer H P, Burgarth D and Petruccione F 2004 *Phys. Rev.* B **70** 045323
Hamdouni Y, Fannes M and Petruccione F 2006 *Phys. Rev.* B **73** 245323
Yuan X Z, Goan H S and Zhu K D 2007 *Phys. Rev.* B **75** 045331

[13] Chiara G D, Fazio R, Macchiavello C, Montangero S and Palma G M 2004 *Phys. Rev.* A **70** 062308
Chen Q, Cheng J H, Wang K L and Du J F 2006 *Phys. Rev.* A **74** 034303

[14] Jiang Z, Chen Q and Wan S L 2007 *Phys. Rev.* A **76** 034302

[15] Hutton A and Bose S 2002 *Phys. Rev.* A **66** 032320

[16] Leibfried D, DeMarco B, Meyer V, Rowe M, Ben-Kish A, Britton J, Itano W M, Jelenković B, Langer C, Rosenband T and Wineland D J 2002 *Phys. Rev. Lett.* **89** 247901
Porras D and Cirac J I 2004 *Phys. Rev. Lett.* **92** 207901

[17] Loss D and Divincenzo D P 1998 *Phys. Rev.* A **57** 120

[18] Imamoğlu A, Awschalom D D, Burkard G, Divincenzo D P, Loss D, Sherwin M and Small A 1999 *Phys. Rev. Lett.* **83** 4204

[19] Hartmann M J, Brandão Fernando G S L and Plenio M B 2007 *Phys. Rev. Lett.* **99** 160501

[20] Angelakis D G, Santos M F and Bose S 2007 *Phys. Rev.* A **76** 031805(R)

[21] Dimer F, Estienne B, Parkins A S and Carmichael H J 2007 *Phys. Rev.* A **75** 013804
Morrison S and Parkins A S 2007 quant-ph/07112325

[22] Yeo Y 2002 *Phys. Rev.* A **66** 062312

[23] Jeong H and Ralph T C 2007 *Phys. Rev.* A **76** 042103

[24] Štelmachovič Peter and Bužek Vladimír 2004 *Phys Rev.* A **70** 032313